crystals

MDPI

Article

Light-Driven Pitch Tuning of Self-Assembled Hierarchical Gratings

Yuan-Hang Wu [1], Sai-Bo Wu [1], Chao Liu [1], Qing-Gui Tan [2], Rui Yuan [1], Jing-Ge Wang [3], Ling-Ling Ma [1,*] and Wei Hu [1]

[1] Key Laboratory of Intelligent Optical Sensing and Manipulation, College of Engineering and Applied Sciences, Nanjing University, Nanjing 210093, China; wuyuanhang163@163.com (Y.-H.W.); cyber0606@163.com (S.-B.W.); by20130678@163.com (C.L.); ruiyuanedu@163.com (R.Y.); huwei@nju.edu.cn (W.H.)
[2] National Key Laboratory of Science and Technology on Space Microwave, Xi'an 710100, China; uestctqg@163.com
[3] Heze Vocational College, Heze 274000, China; wangjingge666@163.com
* Correspondence: malingling@nju.edu.cn; Tel.: +86-25-8359-7400

Abstract: Gratings are of vital importance in modern optics. Self-assembled cholesteric liquid crystal (CLC) gratings have attracted intensive attention due to their easy fabrication and broad applications. However, simultaneously achieving arbitrary patterning and delicate tuning of CLC gratings remains elusive. Here, light-driven pitch tuning is accomplished in hierarchical gratings formed in a molecular switch doped CLC. We fabricate a checkerboard hierarchical CLC grating for a demonstration, whose pitch is optically tuned from 4.6 μm to 10.7 μm. Correspondingly, the first-order diffraction angle continuously changes from 9.4° to 4.8° and a significant polarization selectivity is also observed. In addition, hierarchical CLC gratings with triangular wave pattern, Archimedean spiral, and radial stripes are also demonstrated. This work creates new opportunities for soft-matter-based intelligent functional materials and advanced photonic devices.

Keywords: liquid crystals; gratings; beam steering; photoalignment

Citation: Wu, Y.-H.; Wu, S.-B.; Liu, C.; Tan, Q.-G.; Yuan, R.; Wang, J.-G.; Ma, L.-L.; Hu, W. Light-Driven Pitch Tuning of Self-Assembled Hierarchical Gratings. *Crystals* **2021**, *11*, 326. https://doi.org/10.3390/cryst11040326

Academic Editor: Ingo Dierking

Received: 11 March 2021
Accepted: 22 March 2021
Published: 25 March 2021

1. Introduction

Optical gratings are key components of spectrometers, sensors, tomography, media storage, and beam steering devices widely adopted in nanofabrication, biological medicine, and military areas. Usually, they can be made by physical techniques, such as mechanical ruling, electron beam ablation, lithography, and holography, or by bottom-up chemical nanofabrication [1–4]. However, these methods are often complicated and limited to producing gratings with a fixed grating constant. Liquid crystal (LC), a typical soft building block, has the ability to self-assemble into various hierarchical superstructures [5–7]. Thanks to the high responsiveness to diverse external stimuli, LC gratings have played important roles in tunable optical components for light manipulation [8–10]. Recently, fingerprint textures of cholesteric LC (CLC) have attracted intensive attention due to their controllable pitch of self-organized periodic configurations [11–13]. Vast potentials have been investigated, including nonmechanical beam steering [12], spectrum scanning [14], particle assembly [15], optical vortices generator [16], tunable laser [17], anti-counterfeiting [18], and photolithography [19]. For all these applications, it is a fundamental and key requirement to obtain desired and reliable helical superstructures.

So far, much effort has been devoted to the patterning of helical superstructures and continuous tuning of the fingerprint gratings. Usually, the homogeneously aligned CLC exhibits a unidirectional grating vector [20,21]. In 2007, two-dimensional (2D) diffractive gratings were proposed in photo-responsive dye-doped CLCs [22]. Chen et al. presented interlaced fingerprint textures via sequential UV-induced polymer stabilization [23].

Direction-controllable CLC gratings were further obtained by introducing patterned electrodes or alignments under appropriate electric fields [24,25]. In addition, the vector or pitch of grating can be tuned via changing the helical pitch p with light stimulation, electric field actuation, or concentration regulation [13,14,26–28]. Nevertheless, the above methods are usually complicated; and most reported results are limited to either structure patterning or dynamic tuning of the grating pitch L. If one could realize desired patterning of fingerprint landscapes with tunable L, new functionalities based on smart CLC gratings would be reasonably expected.

In this work, we report a light-driven pitch tuning of hierarchical CLC gratings generated by photopatterning a photo-responsive CLC doped with chiral molecular switches. Upon UV irradiation, the pitch of a checkerboard hierarchical CLC grating presents a continuous increase. The corresponding diffraction regulations are also investigated. Moreover, a triangular wave pattern, an Archimedean spiral, and radial stripes are achieved as well, verifying the flexibility of the photopatterning technique. This work demonstrates the combination of photopatterning and photo-tuning of self-assembled hierarchical gratings, which bring us more possibilities in dynamic functional optics.

2. Materials and Methods

2.1. Materials

The CLC mixture is composed of 99.54 wt.% nematic liquid crystal E7 (Jiangsu Hecheng Display Technology, Nanjing, China) with a positive dielectric anisotropy and 0.46 wt.% left-handed chiral molecular switch ChAD-3C-S (BEAM Company, Orlando, FL, USA). The incorporation of ChAD-3C-S in E7 yields an initial helical twisting power (HTP) of -42.6 μm^{-1} in the dark [29]. Under the irradiation of UV light, HTP decreases due to the transformation of ChAD-3C-S. It shows a reverse change when providing a high ambient temperature or upon green light irradiation [30]. The HTP in green-light photo-stationary state is about -30.7 μm^{-1} [31]. The p of CLC is determined by

$$p = \frac{1}{c \cdot \mathrm{HTP} \cdot ee}, \quad (1)$$

where c and ee are the concentration and the enantiomeric excess of the chiral molecular switch, respectively. Thus, for c = 0.46 wt.%, the initial p is calculated as 5.1 μm (ee = 1) and measured as 3.9 μm. The ps in the UV photo-stationary state and the photo-stationary state achieved by green light exposure are 8.1 μm and 4.8 μm, respectively.

To implement the photopatterning of CLCs, sulfonic azo dye SD1 (Dai-Nippon Ink and Chemicals, Tokyo, Japan) is used as the photoalignment agent, which is dissolved in dimethylformamide (DMF, Sigma-Aldrich, Saint Louis, MO, USA) at the concentration of 0.3 wt.%. SD1 molecules tend to reorient their long axes perpendicular to the incident linear polarization of UV light in order to minimize the photon absorption, thus guiding the alignment of LC molecules [32,33].

2.2. Methods

The CLC cell is assembled with two transparent glass substrates (1.5 × 2 cm^2). Their inner surfaces are coated with indium tin oxide and SD1. The cell thickness d is determined by the spacers (5 μm) between the two substrates and measured as 4.9 μm by the optical interference method. The empty cell is placed at the image plane of the digital micromirror device (DMD, home-made) based micro-lithography system to record the desired in-plane molecular orientations by the photoalignment technique [34]. The CLC mixture is stirred in the isotropic phase (73 °C) and capillary filled into the cell. After the temperature is gradually decreasing to room temperature, a planar cholesteric texture appears and CLC gratings are formed when AC voltage is applied. The textures are observed under a polarized optical microscope (POM) (Nikon 50i, Tokyo, Japan) with an illuminating light of low intensity and recorded by a CCD (Nikon DS-Ri1, Tokyo, Japan). A He-Ne laser (Thorlabs HNLS008L-EC, Newton, MA, USA) at 632.8 nm is used as the probe laser in the

diffraction measurements. The diffraction patterns are captured by a digital camera (Canon EOS 600D, Tokyo, Japan).

3. Results and Discussion

After the CLC mixture is filled in a homogeneously photoaligned cell, the LC molecules self-assemble into a helical structure with helix axes perpendicular to the substrates (Figure 1a). A planar texture in uniform orange is observed under the POM (Figure 1b). When applying an AC voltage,

$$U \geq U_{th} = \pi/p\left\{[k_{11}(p/d)^2 + 4k_{33}]/\Delta\varepsilon\varepsilon_0\right\}^{1/2}, \quad (2)$$

where k_{11}, k_{22} and k_{33} are the splay, twist and bend elastic constants, respectively, ε_0 is the vacuum permittivity and ε is the dielectric anisotropy of the liquid crystal [35], unidirectional stripes begin to grow parallel to the alignment direction. In our experiment, U = 2.5 V (f = 1 kHz). Due to the antagonistic energies between the anchoring energy and helical twisted power, the helix axes are field-induced parallel to the substrates (Figure 1c). Due to the periodic modulation of the refractive index along the helical axis, a one-dimensional phase grating in the Raman–Nath regime is generated with L = 4.9 μm (Figure 1d). For a given cell, L strongly depends on p. When U exceeds 3 V, grating stripes begin to disappear and finally the CLC grating is switched off. A homeotropic nematic-like configuration is also obtained after U reaches 10 V.

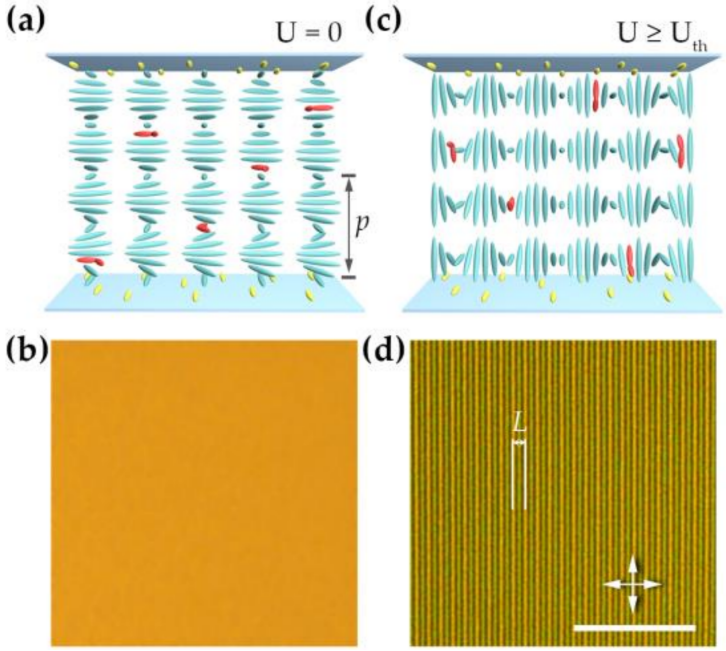

Figure 1. Homogeneously aligned photo-responsive cholesteric liquid crystals (CLCs). (**a**,**c**) Schematic diagrams and (**b**,**d**) corresponding POM images of the planar texture and the electric field-induced grating. The chiral dopants, SD1 and LC molecules are marked by red, yellow and light blue rods, respectively. White arrows denote the transmission axes of polarizer and analyzer. The scale bar is 50 μm.

By means of photoalignment, a 2D checkerboard hierarchical grating is created and a delicate light control is further performed. As shown in Figure 2a, the size of the checkboard unit is 150 μm × 150 μm and the alignment directions in checkerboard units are perpendicular to each other indicated by yellow arrows. When applying a voltage of 2.3 V, orthogonal gratings gradually fill the checkerboard. To investigate the optical tuning property, the checkerboard hierarchical grating is irradiated under UV light (λ = 365 nm, intensity, I = 3 μW cm^{-2}). With the exposure time T increasing from 0 min to 25 min, L is gradually elongated from 4.6 μm to 10.7 μm, which is 2.3 times the initial L (Figure 2b). L

stays almost stable for 40 min after the light is turned off. The corresponding dependency of L on T is presented in Figure 2c. The increase of L originates from the photo-induced transformation of the chiral molecular switch, which reduces the HTP and results in the unwinding of helical structure. After 25-min irradiation, the decreased HTP is not sufficient to maintain stripes. Thus, the CLC grating begins to disappear, leading to a uniform texture with metastable unwound nematic configuration. A reverse optical tuning process is given in Supplementary Materials.

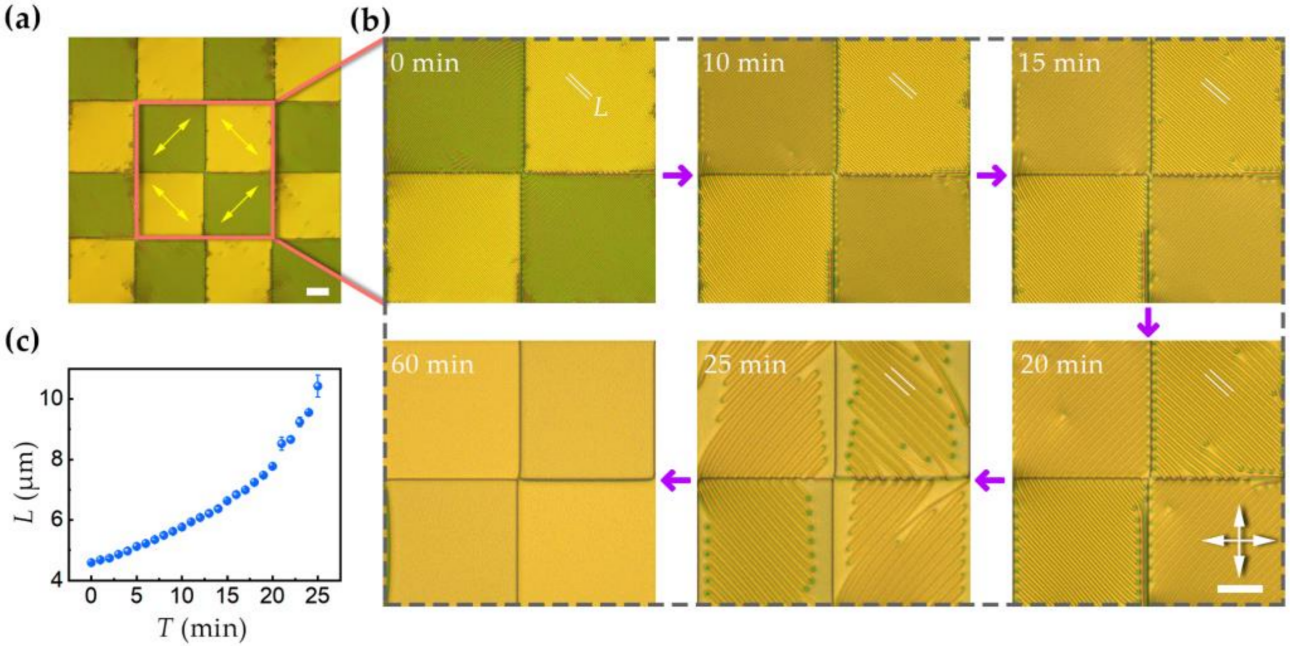

Figure 2. Optical tuning of the checkerboard hierarchical grating. (**a**) POM texture of checkerboard hierarchical grating obtained at 2.3 V, f = 1 kHz. Yellow arrows indicate local alignment directions; (**b**) optical tuning process of the grating under UV exposure. The exposure time is labeled; (**c**) dependency of L on T. White arrows denote the transmission axes of polarizer and analyzer. The scale bars are 50 μm.

To further inspect the performance of CLC hierarchical gratings, a He–Ne laser at 632.8 nm with circular polarization is normally incident onto the cell. The diameter of the probe laser beam is ~ 1 mm. The resultant diffraction pattern is projected onto a screen and captured by a digital camera. The schematic diagram of the light path is shown in Figure 3a. The screen is set to receive diffraction patterns. As shown in Figure 3b, up to fifth-order diffraction spots along the x and y-axis are clearly observed (distance between the sample and the screen, S = 67.75 cm), indicating a large-area and well-ordered checkerboard configuration. The field-induced fingerprint grating diffracts light into four diagonal directions, visible up to the fourth order (S = 5.15 cm). Once the grating is irradiated under UV light, the first-order diffraction angle θ decreases from 9.4° to 4.8° due to the expanding of L (Figure 3c). The excellent regularity of L during light irradiation implies a predictable and reliable method for beam steering. In addition, the polarization sensitivity of the CLC grating is also investigated. As shown in Figure 3d, it is obvious that the spots diffracted from stripes parallel to the incident polarization possess higher intensity than those diffracted from orthogonal stripes, stemming from the optical anisotropy of the LCs and the periodic lying-helix structure inside the CLC grating [16,36,37].

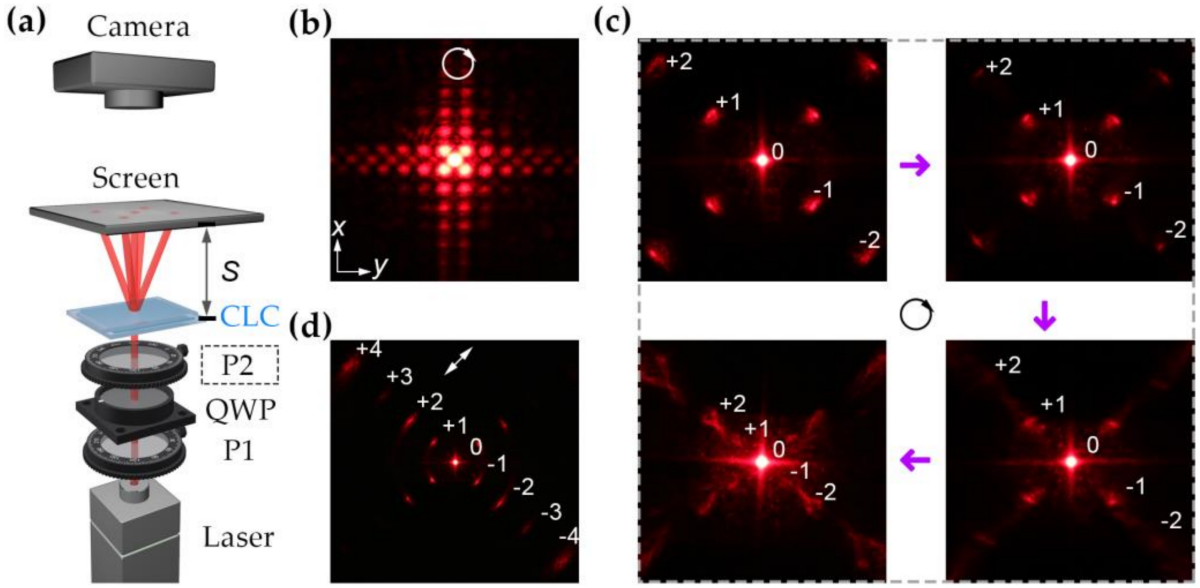

Figure 3. Diffraction performance of checkerboard hierarchical gratings. (**a**) Schematic diagram of the light path. P and QWP represent the polarizer and the quarter wave plate, respectively. P1 and QWP are utilized to produce circularly polarized light. P2 is used to generate linearly polarized light; (**b**) diffraction pattern from the checkerboard hierarchical gratings; (**c**) optical tuning of the diffraction orders at T = 0 min, 5 min, 10 min, and 20 min, respectively; (**d**) polarization-dependent diffraction pattern. Circular and white arrows denote the polarization state of incident light.

Besides checkerboard hierarchical gratings, more complex and photo-responsive CLC hierarchical gratings are fabricated by rationally designing the alignments. As shown in Figure 4a, a micro-pattern of alternating $\pm 45^{\circ}$ alignment is constructed with a two-step photo-exposure process [34]. Consequently, a triangular wave CLC grating is obtained accordingly (Figure 4b). To obtain a continuous space-variant orientation of SD1, the designed LC director distribution is divided into 90 equal subregions, endowed with uniform director values from $\pi/90$ to π in intervals of $\pi/90$. A sum-region of five adjacent subregions is exposed simultaneously with an exposure dose of 1 J cm^{-2}, which is one fifth of the sufficient exposure dose for the reorientation of SD1. The subsequent exposure of the sum-region shifts one subregion with the polarization changing 2° synchronously. After the 90-step five-time partly overlapping exposure, a nearly arbitrary continuously varied alignment can be obtained. Thus, the Archimedean spiral and radial gratings are easily achieved by presetting angular and radial alignments (Figure 4c–f). Their optical tuning performances are similar to the abovementioned checkerboard gratings. It is worth mentioning that the light-induced variation of L is accompanied with the relaxation and unwinding of the Archimedean spiral, due to the limited number of stripes (usually only one stripe).

So far, we have achieved the complex photopatterning of CLC gratings and the light-driven tuning of pitches. The hierarchical architecture of CLCs in the checkerboard grating originates from three distinct levels. One is the self-assembled helical structure and the other two are the field-induced fingerprint gratings and the periodic checkerboard pattern introduced by the photoalignment technique. Thanks to the intrinsic self-assembly of CLC, the photopatterned CLC gratings show the merits of simple-fabrication, reconfigurable, cost-efficiency, and easy-miniaturization. The photo-responsive chiral molecular switch induces the winding/unwinding of CLC helices and subsequently tunes the pitches of generated gratings. A drastic tuning range of 4.6 μm to 10.7 μm is achieved. The pitch tuning and beam steering exhibit a delicate, remote, and reversible control, which is promising in various active diffraction elements. It only needs a stimulating UV light with weak intensity of ~ 3 μW cm^{-2}, which can be supplied by an incoherent light-emitting diode and eliminates the light damage to the sample [38]. In addition to the light controllability, the three-dimensional architecture of directors can be multi-manipulated by combining

different stimuli, including heat, magnetic, and acoustic fields. Although only growing-modulation type fingerprints are demonstrated here, more fruitful complex gratings can be reasonably expected by introducing developable-modulation type fingerprints, whose formation is similar to the development of a photograph [39].

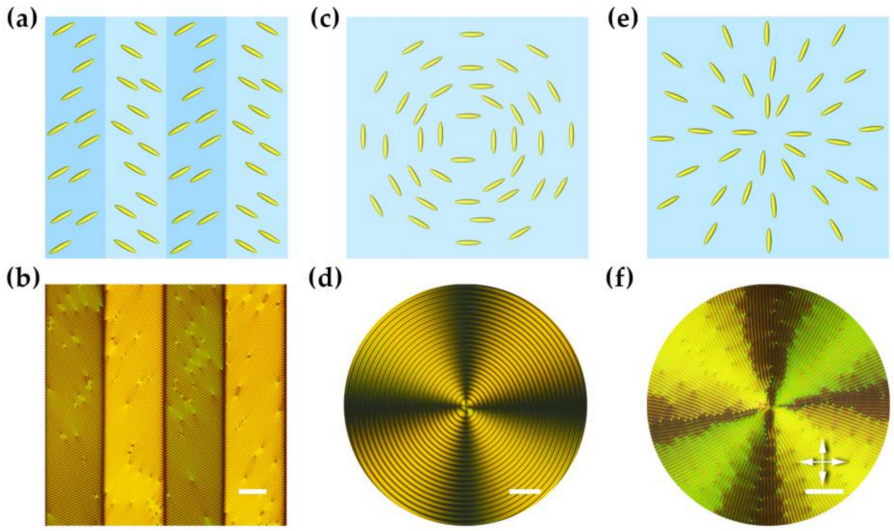

Figure 4. Photopatterned CLC gratings. (**a**,**c**,**e**) Schematic diagrams of binary, radial and angular alignments; (**b**,**d**,**f**) corresponding images of fingerprint textures. SD1 molecules are represented by yellow bars. White arrows denote the polarizer transmission axes. All scale bars indicate 50 μm.

4. Conclusions

In conclusion, we propose electrically induced, photopatterned, and optically tuned hierarchical CLC gratings in a photosensitive helical medium. A checkerboard grating is photopatterned and optically tuned, providing a continuous L tuning from 4.6 μm to 10.7 μm. The corresponding beam steering capability is also investigated. Furthermore, a triangular wave pattern, an Archimedean spiral, and radial fingerprint gratings are also demonstrated thanks to the flexibility of the photopatterning technique. This work will open a new approach for fantastic, dynamic, and intelligent optical devices that may be widely utilized in beam steering, virtual reality, measurements, optical data storage, communications, etc.

Supplementary Materials: The following are available online at https://www.mdpi.com/2073-4352/11/4/326/s1, Figure S1: Reverse optical pitch tuning process of the checkerboard hierarchical grating upon the irradiation of green light.

Author Contributions: L.-L.M. and W.H. conceived the original idea; Y.-H.W. and L.-L.M. performed the experiments, analyzed the data and wrote the manuscript with the assistance of S.-B.W., C.L., Q.-G.T., R.Y. and J.-G.W.; L.-L.M. directed the research. All authors have read and agreed to the published version of the manuscript.

Funding: This research was funded by the National Natural Science Foundation of China (NSFC), grant number 62035008, 52003115 and 61922038, National Key Laboratory Foundation of China, grant number 6142411195411, and Natural Science Foundation of Jiangsu Province, grant number BK20200320.

Acknowledgments: This work was also supported by the Innovation and Entrepreneurship Program of Jiangsu Province. The authors gratefully appreciate Hao Qian (Nanjing Tech University), Cong-Long Yuan (East China University of Science and Technology), Chao-Yi Li (Nanjing University) and Yi-Heng Zhang (Nanjing University) for their constructive discussions.

Conflicts of Interest: The authors declare no conflict of interest.

References

1. Kuppe, C.; Williams, C.; You, J.; Collins, J.T.; Gordeev, S.N.; Wilkinson, T.D.; Panoiu, N.-C.; Valev, V.K. Circular dichroism in higher-order diffraction beams from chiral quasiplanar nanostructures. *Adv. Opt. Mater.* **2018**, *6*, 1800098. [CrossRef]
2. Espinha, A.; Dore, C.; Matricardi, C.; Alonso, M.I.; Goni, A.R.; Mihi, A. Hydroxypropyl cellulose photonic architectures by soft nanoimprinting lithography. *Nat. Photonics* **2018**, *12*, 343–348. [CrossRef]
3. Yu, C.; O'Brien, K.; Zhang, Y.-H.; Yu, H.; Jiang, H. Tunable optical gratings based on buckled nanoscale thin films on transparent elastomeric substrates. *Appl. Phys. Lett.* **2010**, *96*, 041111. [CrossRef]
4. Ryabchun, A.; Wegener, M.; Gritsai, Y.; Sakhno, O. Novel effective approach for the fabrication of pdms-based elastic volume gratings. *Adv. Opt. Mater.* **2015**, *4*, 169–176. [CrossRef]
5. Bisoyi, H.K.; Li, Q. Light-directing chiral liquid crystal nanostructures: From 1d to 3d. *Acc. Chem. Res.* **2014**, *47*, 3184–3195. [CrossRef] [PubMed]
6. Ma, L.L.; Tang, M.J.; Hu, W.; Cui, Z.Q.; Ge, S.J.; Chen, P.; Chen, L.J.; Qian, H.; Chi, L.F.; Lu, Y.Q. Smectic layer origami via preprogrammed photoalignment. *Adv. Mater.* **2017**, *29*, 1606671. [CrossRef] [PubMed]
7. Ma, L.-L.; Hu, W.; Zheng, Z.-G.; Wu, S.-B.; Chen, P.; Li, Q.; Lu, Y.-Q. Light-activated liquid crystalline hierarchical architecture toward photonics. *Adv. Opt. Mater.* **2019**, *7*, 1900393. [CrossRef]
8. Guglielmelli, A.; Nemati, S.; Vasdekis, A.E.; De Sio, L. Stimuli responsive diffraction gratings in soft-composite materials. *J. Phys. D Appl. Phys.* **2019**, *52*, 053001. [CrossRef]
9. Ma, Y.; Wang, X.; Srivastava, A.K.; Chigrinov, V.G.; Kwok, H.S. Fast switchable ferroelectric liquid crystal gratings with two electro-optical modes. *AIP Adv.* **2016**, *6*, 035207. [CrossRef]
10. Ma, Y.; Wei, B.Y.; Shi, L.Y.; Srivastava, A.K.; Chigrinov, V.G.; Kwok, H.S.; Hu, W.; Lu, Y.Q. Fork gratings based on ferroelectric liquid crystals. *Opt. Express* **2016**, *24*, 5822–5828. [CrossRef]
11. Ryabchun, A.; Yakovlev, D.; Bobrovsky, A.; Katsonis, N. Dynamic diffractive patterns in helix-inverting cholesteric liquid crystals. *ACS Appl. Mater. Interfaces* **2019**, *11*, 10895–10904. [CrossRef]
12. Ryabchun, A.; Bobrovsky, A. Cholesteric liquid crystal materials for tunable diffractive optics. *Adv. Opt. Mater.* **2018**, *6*, 1800335. [CrossRef]
13. Ryabchun, A.; Bobrovsky, A.; Stumpe, J.; Shibaev, V. Rotatable diffraction gratings based on cholesteric liquid crystals with phototunable helix pitch. *Adv. Opt. Mater.* **2015**, *3*, 1273–1279. [CrossRef]
14. Jau, H.C.; Li, Y.; Li, C.C.; Chen, C.W.; Wang, C.T.; Bisoyi, H.K.; Lin, T.H.; Bunning, T.J.; Li, Q. Light-driven wide-range nonmechanical beam steering and spectrum scanning based on a self-organized liquid crystal grating enabled by a chiral molecular switch. *Adv. Opt. Mater.* **2015**, *3*, 166–170. [CrossRef]
15. Mitov, M.; Portet, C.; Bourgerette, C.; Snoeck, E.; Verelst, M. Long-range structuring of nanoparticles by mimicry of a cholesteric liquid crystal. *Nat. Mater.* **2002**, *1*, 229–231. [CrossRef] [PubMed]
16. Voloschenko, D.; Lavrentovich, O.D. Optical vortices generated by dislocations in a cholesteric liquid crystal. *Opt. Lett.* **2000**, *25*, 317–319. [CrossRef] [PubMed]
17. Huang, W.; Yuan, C.-L.; Shen, D.; Zheng, Z.-G. Dynamically manipulated lasing enabled by a reconfigured fingerprint texture of a cholesteric self-organized superstructure. *J. Mater. Chem. C* **2017**, *5*, 6923–6928. [CrossRef]
18. Li, W.-S.; Shen, Y.; Chen, Z.-J.; Cui, Q.; Li, S.-S.; Chen, L.-J. Demonstration of patterned polymer-stabilized cholesteric liquid crystal textures for anti-counterfeiting two-dimensional barcodes. *Appl. Opt.* **2017**, *56*, 601–606. [CrossRef]
19. Jeong, H.S.; Kim, Y.H.; Lee, J.S.; Kim, J.H.; Srinivasarao, M.; Jung, H.T. Chiral nematic fluids as masks for lithography. *Adv. Mater.* **2012**, *24*, 381–384. [CrossRef]
20. Wu, J.-J.; Wu, Y.-S.; Chen, F.-C.; Chen, S.-H. Formation of phase grating in planar aligned cholesteric liquid crystal film. *Jpn. J. Appl. Phys.* **2002**, *41*, L1318–L1320. [CrossRef]
21. Wu, J.-J.; Chen, F.-C.; Wu, Y.-S.; Chen, S.-H. Phase gratings in pretilted homeotropic cholesteric liquid crystal films. *Jpn. J. Appl. Phys.* **2002**, *41*, 6108–6109. [CrossRef]
22. Yeh, H.-C.; Chen, G.-H.; Lee, C.-R.; Mo, T.-S. Photoinduced two-dimensional gratings based on dye-doped cholesteric liquid crystal films. *J. Chem. Phys.* **2007**, *127*, 141105. [CrossRef]
23. Li, W.-S.; Ma, L.-L.; Gong, L.-L.; Li, S.-S.; Yang, C.; Luo, B.; Hu, W.; Chen, L.-J. Interlaced cholesteric liquid crystal fingerprint textures via sequential uv-induced polymer-stabilization. *Opt. Mater. Express* **2016**, *6*, 19–28. [CrossRef]
24. Yao, I.A.; Liaw, C.-H.; Chen, S.-H.; Wu, J.-J. Direction-tunable cholesteric phase gratings. *J. Appl. Phys.* **2004**, *96*, 1760–1762. [CrossRef]
25. Ma, L.-L.; Li, S.-S.; Li, W.-S.; Ji, W.; Luo, B.; Zheng, Z.-G.; Cai, Z.-P.; Chigrinov, V.; Lu, Y.-Q.; Hu, W.; et al. Rationally designed dynamic superstructures enabled by photoaligning cholesteric liquid crystals. *Adv. Opt. Mater.* **2015**, *3*, 1691–1696. [CrossRef]
26. Zheng, Z.-G.; Li, Y.; Bisoyi, H.K.; Wang, L.; Bunning, T.J.; Li, Q. Three-dimensional control of the helical axis of a chiral nematic liquid crystal by light. *Nature* **2016**, *531*, 352–356. [CrossRef] [PubMed]
27. Cao, Y.; Wang, P.X.; D'Acierno, F.; Hamad, W.Y.; Michal, C.A.; MacLachlan, M.J. Tunable diffraction gratings from biosourced lyotropic liquid crystals. *Adv. Mater.* **2020**, *32*, 1907376. [CrossRef]
28. Hamdi, R.; Petriashvili, G.; De Santo, M.; Lombardo, G.; Barberi, R. Electrically controlled 1d and 2d cholesteric liquid crystal gratings. *Mol. Cryst. Liq. Cryst.* **2012**, *553*, 97–102. [CrossRef]

29. Chen, C.-W.; Li, C.-C.; Jau, H.-C.; Lee, C.-H.; Wang, C.-T.; Lin, T.-H. Bistable light-driven π phase switching using a twisted nematic liquid crystal film. *Opt. Express* **2014**, *22*, 12133–12138. [CrossRef] [PubMed]
30. Hsiao, Y.-C.; Huang, K.-C.; Lee, W. Photo-switchable chiral liquid crystal with optical tristability enabled by a photoresponsive azo-chiral dopant. *Opt. Express* **2017**, *25*, 2687–2693. [CrossRef] [PubMed]
31. Huang, K.C.; Hsiao, Y.C.; Timofeev, I.V.; Zyryanov, V.Y.; Lee, W. Photo-manipulated photonic bandgap devices based on optically tristable chiral-tilted homeotropic nematic liquid crystal. *Opt. Express* **2016**, *24*, 25019–25025. [CrossRef]
32. Hu, W.; Kumar Srivastava, A.; Lin, X.W.; Liang, X.; Wu, Z.J.; Sun, J.T.; Zhu, G.; Chigrinov, V.G.; Lu, Y.Q. Polarization independent liquid crystal gratings based on orthogonal photoalignments. *Appl. Phys. Lett.* **2012**, *100*, 111116. [CrossRef]
33. Wu, H.; Hu, W.; Hu, H.C.; Lin, X.W.; Zhu, G.; Choi, J.W.; Chigrinov, V.G.; Lu, Y.Q. Arbitrary photo-patterning in liquid crystal alignments using dmd based lithography system. *Opt. Express* **2012**, *20*, 16684–16689. [CrossRef]
34. Wei, B.-Y.; Hu, W.; Ming, Y.; Xu, F.; Rubin, S.; Wang, J.-G.; Chigrinov, V.G.; Lu, Y.-Q. Generating switchable and reconfigurable optical vortices via photopatterning of liquid crystals. *Adv. Mater.* **2014**, *26*, 1590–1595. [CrossRef]
35. van Sprang, H.A.; van de Venne, J.L.M. Influence of the surface interaction on threshold values in the cholesteric-nematic phase transition. *J. Appl. Phys.* **1985**, *57*, 175–179. [CrossRef]
36. Subacius, D.; Bos, P.J.; Lavrentovich, O.D. Switchable diffractive cholesteric gratings. *Appl. Phys. Lett.* **1997**, *71*, 1350–1352. [CrossRef]
37. Hung, W.-C.; Cheng, W.-H.; Liu, T.-K.; Jiang, I.M.; Tsai, M.-S.; Yeh, P. Diffraction of cholesteric liquid crystal gratings probed by monochromatic light from 450 to 750 nm. *J. Appl. Phys.* **2008**, *104*, 073106. [CrossRef]
38. Yada, M.; Yamamoto, J.; Yokoyama, H. Direct observation of anisotropic interparticle forces in nematic colloids with optical tweezers. *Phys. Rev. Lett.* **2004**, *92*, 185501. [CrossRef]
39. Fuh, A.Y.-G.; Lin, C.-H.; Huang, C.-Y. Dynamic pattern formation and beam-steering characteristics of cholesteric gratings. *Jpn. J. Appl. Phys.* **2002**, *41*, 211–218. [CrossRef]